

## Resonant tunneling between thermal excited states tuned by a magnetic field

G. S. Vieira,<sup>1,\*</sup> W. H. M. Feu,<sup>2</sup> J. M. Villas-Bôas,<sup>1,2</sup> P. S. S. Guimarães,<sup>2</sup> and Nelson Studart<sup>3</sup>

<sup>1</sup>*Divisão de Física Aplicada, Instituto de Estudos Avançados, 12228-001 São José dos Campos, São Paulo, Brazil*

<sup>2</sup>*Departamento de Física, Universidade Federal de Minas Gerais, 30123-970 Belo Horizonte, Minas Gerais, Brazil*

<sup>3</sup>*Departamento de Física, Universidade Federal de São Carlos, 13565-905 São Carlos, São Paulo, Brazil*

(Received 19 December 2006; revised manuscript received 9 March 2007; published 18 May 2007)

In this Brief Report, we present temperature-dependent magnetotransport measurements in a coupled multi-quantum-well structure in the presence of a magnetic field applied parallel to the layers. We use the magnetic field to tune into resonance a thermally occupied excited subband in one well with a lower energy subband in an adjacent well, increasing the tunneling rates. The result is shown as additional structures in the current versus magnetic-field curves as the temperature increases.

DOI: [10.1103/PhysRevB.75.193406](https://doi.org/10.1103/PhysRevB.75.193406)

PACS number(s): 73.21.Cd, 73.40.Gk, 73.63.Hs

Over the past decades, resonant-tunneling semiconductor structures have been widely used for studying fundamental physical processes as well as for developing novel electro-optical devices. Most of the early studies were focused on double-barrier resonant-tunneling diodes,<sup>1</sup> which were followed by coupled multi-quantum-wells (MQWs) and superlattice (SL) structures.<sup>2–4</sup> Under a bias voltage, electrons can tunnel through the barriers and wells of the structure, and by continuously changing the bias, a number of peaks can be seen in the current-voltage ( $I$ - $V$ ) characteristics. A magnetic field applied parallel to the layers ( $x$  direction) of the structure leads to the formation of electric-magnetic subbands for both electrons and holes<sup>5–7</sup> and modifies the resonant-tunneling conditions.<sup>8</sup> This effect has been used to probe the electron and hole wave functions in semiconductor nanostructures in what has been called magnetotunneling spectroscopy.<sup>9–11</sup> For small magnetic fields, perturbation theory is valid and the effects are a slight increase of the bound-state electron energy in the wells and a small shift in the energy dispersion relations.<sup>12</sup> For a high enough magnetic field, the electric subbands change to magnetic ones. The magnetic quantization in superlattices was earlier reviewed by Maan.<sup>12</sup> An important result is that states at the anticrossings of the subband dispersion relations dependent on the wave vector  $k_y$  (the growth direction is  $z$ ) constitute new tunneling channels.<sup>8,13–15</sup> Furthermore, if the electrons are in thermal equilibrium inside each subband, the tunneling channels that are better observed in transport measurements will be those close to the bottom of the occupied subbands.<sup>16</sup> The magnetic field gradually suppresses the hysteresis of  $I$ - $V$  characteristics in the coupled MQWs.<sup>17</sup> At high enough magnetic fields, the steplike  $I$ - $V$  curve of a coupled MQWs becomes smooth due to the broadening of tunneling resonances.<sup>18</sup> The current versus magnetic field ( $I$ - $B$ ) curves at low bias typically show a maximum in current for both weakly<sup>19</sup> and strongly coupled SLs.<sup>20</sup> In the latter case, the maximum depends on both applied bias and miniband width.<sup>20</sup>

In a previous work,<sup>21</sup> resonant electron tunneling from the bottom of the second energy subband of a given well into the first energy subband of the adjacent well tuned with a parallel magnetic field was observed. Electron tunneling without intrasubband energy relaxation was also seen. In the experi-

ment, electrons were photoexcited from first to second subband by applying THz radiation. Here, we show that the first effect, i.e., resonant electron tunneling from the bottom of the second energy subband of a given well into the first subband of the adjacent well, can be obtained by thermal occupation of the excited subbands. The tunneling channel is revealed as an extra peak in the  $I$ - $B$  curve that increases as the temperature increases. By raising the temperature even further, resonant magnetically tuned tunneling from the bottom of higher subbands was also observed.

The sample used in this work was grown by molecular-beam epitaxy over a semi-insulating GaAs substrate. It consists of a coupled MQW structure made of ten layers of GaAs and 11 layers of  $\text{Al}_{0.3}\text{Ga}_{0.7}\text{As}$  sandwiched between two layers of GaAs, each 50 nm thick. All these layers are uniformly doped with Si to  $3 \times 10^{15} \text{ cm}^{-3}$ . This structure was again sandwiched between two 300-nm-thick GaAs layers heavily doped with Si to  $2 \times 10^{18} \text{ cm}^{-3}$ . The nominal thicknesses of the GaAs wells and  $\text{Al}_{0.3}\text{Ga}_{0.7}\text{As}$  barriers are 33 and 4 nm, respectively. In a previous work with the same sample,<sup>22</sup> the resonance frequency of the first intersubband transition, at zero magnetic field, was measured as  $3.27 \pm 0.05$  THz. Comparing this value with a simple envelope function calculation for an isolated well, the real width of the wells was assumed to be 31.7 nm. The magnetic field was always applied parallel to the layers (perpendicular to the current).

Using the effective-mass approximation, the Hamiltonian for one electron, with effective mass  $m^*$  and charge  $-e$ , in the conduction band of the coupled MQW in the presence of a magnetic field  $B$  along the  $x$  direction and an electric field  $F$  along the  $z$  direction can be written as

$$H = \frac{p_x^2}{2m^*} + \frac{m^* \omega_c^2}{2} \left( \frac{p_y}{eB} - z \right)^2 + \frac{p_z^2}{2m^*} - eFz + U(z), \quad (1)$$

where the vector potential is  $\vec{A} = (0, -zB, 0)$ ,  $U(z)$  describes the MQW potential profile,  $\mathbf{p}$  is the canonical momentum, and  $\omega_c = (eB/m^*)$  is the cyclotron frequency.

In order to understand the features of the tunneling processes, we have calculated the energy subbands by obtaining a full numerical solution of the Schrödinger equation associated with the Hamiltonian (1) through the expansion of the

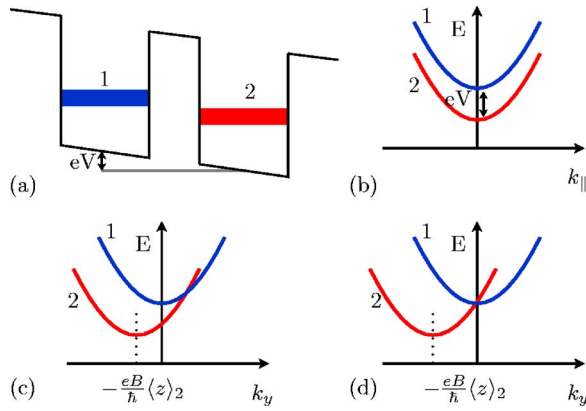


FIG. 1. (Color online) (a) First energy subbands in adjacent wells under a small electric field. (b) Schematic energy dispersion curves of both  $k_y$  and  $k_x$  for two subbands, located in adjacent wells, without an applied magnetic field. (c) Schematic energy dispersion curves of  $k_y$  for the same two subbands at a nonvanishing magnetic field. The term  $\langle z \rangle_1$  was set to zero for simplicity. (d) The same two subbands for a magnetic field at which the crossing between the two subbands occurs at the bottom of the highest energy subband.

Hamiltonian on the basis of an infinite square well much larger than the MQW region and then solving the resulting eigenvalue problem for different  $k_y$  and  $B$  values.<sup>21</sup> It is well known that the Hamiltonian (1) leads to shifted parabolic  $k_y$  energy dispersions which have minima at  $(k_y)_{\min}$  dependent on each subband.<sup>23</sup> Qualitatively, this result can be interpreted using a classical argument by momentum conservation upon tunneling. When tunneling between adjacent wells, the electron, due to the Lorentz force, acquires the momentum  $p_y = -eBd$ , where  $d$  is a characteristic tunneling distance. For moderate  $B$ , in first-order perturbation theory, the minimum for the  $n$  subband of a given well is given by  $(k_y)_{\min} = -(eB/\hbar)\langle z \rangle_n$ , where  $\langle z \rangle_n$  is the expectation value for the unperturbed wave function.<sup>12,16</sup>

This fact is especially important for subbands located in different wells [Fig. 1(a)] because it makes the tunneling probability dependent on  $k_y$ , unlike the situation without the magnetic field, where the tunneling is independent of both  $k_y$  and  $k_x$ . Without the magnetic field, and with a small electric field applied, the different subbands on the left and right wells are always out of resonance as in Fig. 1(b), making the tunneling less favorable. On the other hand, when the magnetic field is applied, the different subbands on the left and right wells will present a resonant condition for a special value of  $k_y$ , as they have been displaced by  $-\frac{eB}{\hbar}(\langle z \rangle_2 - \langle z \rangle_1)$  [see Figs. 1(c) and 1(d)].<sup>16</sup> Our numerical solution shows that the crossing between any two dispersion curves of subbands in adjacent wells becomes an anticrossing and the states with  $k_y$  around that value become extended over the two adjacent wells, which is expected.<sup>13,15</sup>

The two wells shown in Fig. 1(a) may represent any two adjacent wells of a MQW structure under a small applied bias. If the electrons are in thermal equilibrium inside each subband, the highest density of electrons should be located around the minimum of the  $k_y$  dispersion. Then, for a fixed bias, the highest tunneling current should occur for a mag-

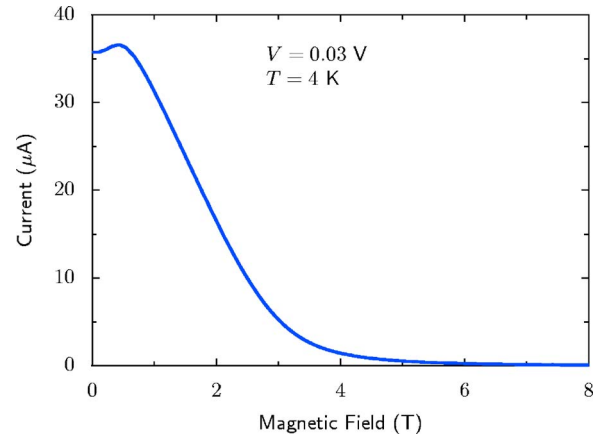


FIG. 2. (Color online) Current versus magnetic field ( $I$ - $B$ ) at a fixed bias of 30 mV and sample temperature of 4 K. At this voltage, the electric field is expected to be uniform over the entire coupled MQW structure. The maximum observed in the current at  $B \approx 0.5$  T is related to the anticrossing between the bottom of the first energy subband of one well with the first energy subband of an adjacent well.

netic field which generates an anticrossing between the two dispersion curves at the minimum of the higher energy one,<sup>16,18</sup> as drawn in Fig. 1(d). If only the lowest electron subband of each well is occupied, an  $I$ - $B$  curve at a fixed low voltage will show a maximum at a relatively low magnetic field, and for higher magnetic fields, the current should then decrease monotonically, dropping asymptotically to zero at high enough fields. Figure 2 shows such an  $I$ - $B$  curve for our sample. Since the voltage drop in the contact region is unknown, the position of this low magnetic-field peak cannot be clearly related to the applied bias.

At a higher magnetic field there will be an anticrossing between the first subband of a given well and the bottom of the second subband of the adjacent wells. The  $k_y$  dispersion curves for three adjacent wells at a magnetic field that fulfills this condition are shown in Fig. 3. The states at the anticrossing are extended over the adjacent wells and tunneling should then be enhanced. To see such effect, in our previous paper<sup>21</sup> we used resonant THz optical pumping to increase the population of the second subband. As a result, we observed a peak in the photocurrent at the magnetic field fulfilling the above condition,  $B = 3.1$  T. In the same paper,<sup>21</sup> we also showed that electrons may be pumped directly to the anticrossing between dispersion curves away from the bottom of any subband, opening a tunneling channel without intrasubband relaxation. This second effect can only be observed by optically pumping the electrons, but the tunneling process from the bottom of the second subband at  $B = 3.1$  T could, in principle, be observed in magnetotransport measurements by just raising the sample temperature, and so, populating the second subband. It should show up as a shoulder in the  $I$ - $B$  curves taken at low bias, as the temperature increases. At low temperatures, there is not a significant number of electrons at the second subband, and nothing is seen in the  $I$ - $B$  curve of Fig. 2 at  $B = 3.1$  T, only the monotonic decrease of current, as expected.

Figure 4(a) shows a sequence of  $I$ - $B$  curves, at the same

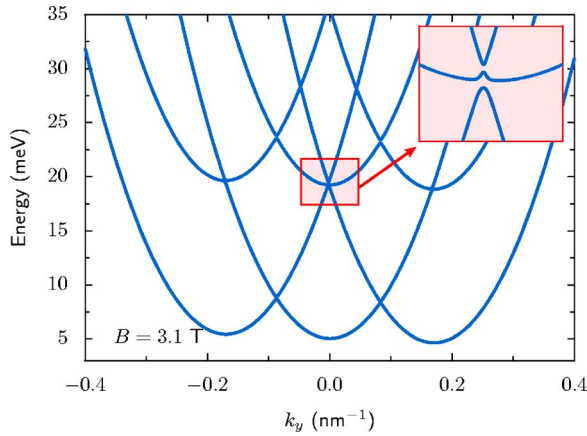


FIG. 3. (Color online)  $k_y$  dispersion curves for a three-well structure using the same parameters of our sample, with an applied magnetic field of 3.1 T and a voltage drop of 0.4 mV per period, calculated numerically in the effective-mass approximation. Inset: amplification of the anticrossing region.

low bias, taken at different sample temperatures. It can be seen that, as the temperature rises, the whole current increases and a shoulder appears in the  $I$ - $B$  curves around the expected magnetic-field value,  $B=3.1$  T. For better identification of the superimposed peak, we have subtracted a linear background from each  $I$ - $B$  curve. The result is shown in Fig. 4(b), where we can clearly see a peak rising with temperature

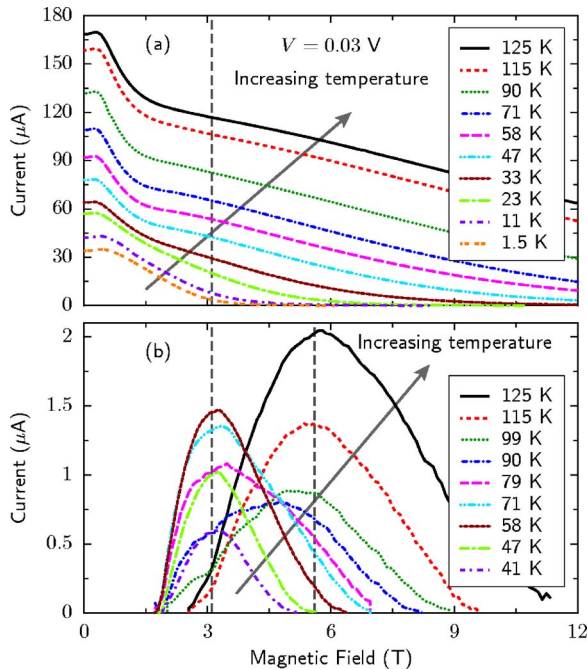


FIG. 4. (Color online) (a) Current versus magnetic field curves taken at different sample temperatures and with the same low bias,  $V=0.03$  V. As we increase the temperature, a shoulder shows up at  $B \approx 3.1$  T (vertical dashed line). (b) Current versus magnetic field curves at different temperatures after background subtraction. The dashed vertical lines represent the expected positions in magnetic field,  $B=3.1$  T and  $B=5.6$  T, for resonant thermal-assisted tunneling.

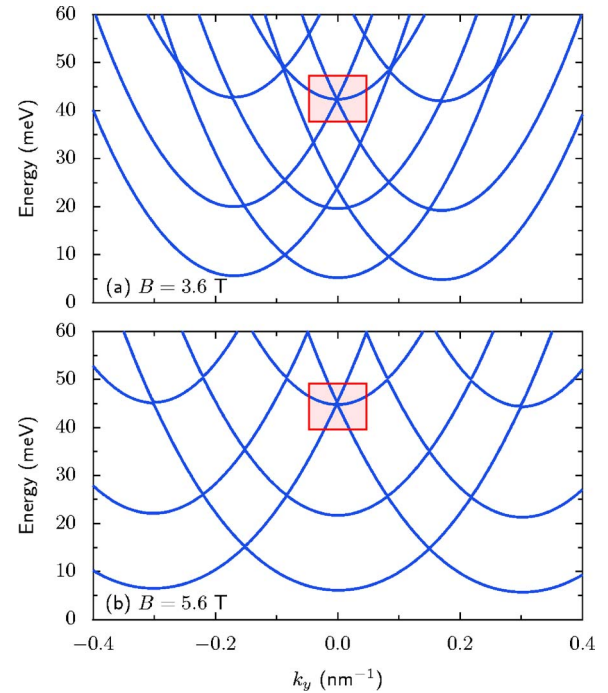


FIG. 5. (Color online) Numerically computed dispersion curves of three adjacent wells for the magnetic field that produces an anticrossing, highlighted by a square, between the bottom of the third energy subband of one well with (a) the second subband ( $B=3.6$  T) and (b) the first subband ( $B=5.6$  T) of the adjacent wells.

up to  $\sim 60$  K for  $B \approx 3.1$  T. The peak broadens gradually with temperature, and as we further increase the temperature, another maximum in the current develops around  $B=5.7$  T.

In order to understand this second peak in the  $I$ - $B$  curves at high temperatures, in Figs. 5(a) and 5(b) we show the numerically computed dispersion curves for three quantum wells with the same parameters of our sample, as in Fig. 3, at magnetic-field intensities at which there is an anticrossing between the bottom of the third subband of a given well and, respectively, the second ( $B=3.6$  T) and the first subband ( $B=5.6$  T) of the adjacent wells.

Figure 5(b) shows that the crossing between the bottom of the third subband of a given well and the first subband of adjacent wells occurs nearly at the same magnetic field,  $B \approx 5.6$  T, at which a peak is seen in the  $I$ - $B$  curves at the highest temperatures measured [ $T \geq 90$  K, Fig. 4(b)]. Therefore, the origin of this maximum in the  $I$ - $B$  curves at high temperature is the magnetic-field-induced onset of tunneling between the bottom of the third energy subband of one quantum well and the first subband of the adjacent wells. This mechanism is possible at high temperatures due to the thermal increase of electron population in the third energy subbands.

According to the results shown in Fig. 5(a), a peak should also be seen in the  $I$ - $B$  curves at  $B=3.6$  T at high temperature ( $T \geq 90$  K), corresponding to the crossing between the bottom of the thermally populated third subband of a given quantum well and the second subband of the adjacent wells. However, this resonance is close to  $B=3.1$  T, where, as

discussed above, the tunneling is enhanced. The overall result as the temperature is increased is then a further broadening of the peak in the  $I$ - $B$  curves at  $B=3.1$  T. Perusal of Fig. 4(b) reveals this broadening, around  $T\sim 80$ – $100$  K. For even higher temperature, the peak centered around  $B\sim 3$ – $4$  T becomes so broad that it is eliminated by the background subtraction used to obtain the curves in Fig. 4(b). It should also be noted that the increase in phonon scattering as the temperature rises, apart from increasing the occupation probability of excited subbands, could also produce additional features in the  $I$ - $V$  or  $I$ - $B$  curves due to phonon-assisted tunneling. However, since the probability for this process is small due to the relatively thick tunneling barriers, we do not see any evidence of it.

To conclude, in this Brief Report, we show that it is possible to observe resonant tunneling from thermally occupied excited subbands to a lower energy subband of coupled multi-quantum-wells in the presence of a magnetic field parallel to the quantum-well layers. Therefore, as the temperature of the sample is increased in the presence of an applied magnetic field, new tunneling mechanisms have to be considered.

The authors gratefully acknowledge S. J. Allen, K. L. Campman, and A. C. Gossard, University of California at Santa Barbara, who provided the samples used in this work. Financial support for this work was provided by FINEP (CT Aeronáutico), FAPEMIG, and CNPq, Brazil.

---

\*Electronic address: gvieira@ieav.cta.br

- <sup>1</sup>L. L. Chang, L. Esaki, and R. Tsu, *Appl. Phys. Lett.* **24**, 593 (1974).
- <sup>2</sup>L. Esaki and L. L. Chang, *Phys. Rev. Lett.* **33**, 495 (1974).
- <sup>3</sup>F. Capasso, K. Mohammed, and A. Y. Cho, *Appl. Phys. Lett.* **48**, 478 (1986).
- <sup>4</sup>K. K. Choi, B. F. Levine, R. J. Malik, J. Walker, and C. G. Bethea, *Phys. Rev. B* **35**, 4172 (1987).
- <sup>5</sup>G. Belle, J. C. Maan, and G. Weimann, *Surf. Sci.* **170**, 611 (1986).
- <sup>6</sup>M. Altarelli and G. Platero, *Surf. Sci.* **196**, 540 (1988).
- <sup>7</sup>G. Platero and M. Altarelli, *Phys. Rev. B* **39**, 3758 (1989).
- <sup>8</sup>L. Brey, G. Platero, and C. Tejedor, *Phys. Rev. B* **38**, 9649 (1988).
- <sup>9</sup>R. K. Hayden, D. K. Maude, L. Eaves, E. C. Valadares, M. Henini, F. W. Sheard, O. H. Hughes, J. C. Portal, and L. Cury, *Phys. Rev. Lett.* **66**, 1749 (1991).
- <sup>10</sup>P. H. Beton, J. Wang, N. Mori, L. Eaves, P. C. Main, T. J. Foster, and M. Henini, *Phys. Rev. Lett.* **75**, 1996 (1995).
- <sup>11</sup>A. Patane, R. J. A. Hill, L. Eaves, P. C. Main, M. Henini, M. L. Zambrano, A. Levin, N. Mori, C. Hamaguchi, Yu. V. Dubrovskii, E. E. Vdovin, D. G. Austing, S. Tarucha, and G. Hill, *Phys. Rev. B* **65**, 165308 (2002).
- <sup>12</sup>J. C. Maan, in *Festkörperprobleme 27*, edited by P. Grosse (Vieweg, Barunschweig, 1987), p. 137.
- <sup>13</sup>G. Platero, L. Brey, and C. Tejedor, *Phys. Rev. B* **40**, 8548 (1989).
- <sup>14</sup>T. M. Fromhold, F. W. Sheard, and G. A. Toombs, *Surf. Sci.* **228**, 437 (1990).
- <sup>15</sup>M. Helm, F. M. Peeters, P. England, J. R. Hayes, and E. Colas, *Phys. Rev. B* **39**, 3427 (1989).
- <sup>16</sup>W. Müller, H. T. Grahn, K. von Klitzing, and K. Ploog, *Phys. Rev. B* **48**, 11176 (1993).
- <sup>17</sup>B. Sun, J. Wang, and D. Jiang, *Semicond. Sci. Technol.* **20**, 947 (2005).
- <sup>18</sup>K. K. Choi, B. F. Levine, N. Jarosik, J. Walker, and R. Malik, *Phys. Rev. B* **38**, 12362 (1988).
- <sup>19</sup>H. T. Grahn, R. J. Haug, W. Müller, and K. Ploog, *Phys. Rev. Lett.* **67**, 1618 (1991).
- <sup>20</sup>F. Aristone, A. Sibille, J. F. Palmier, D. K. Maude, J. C. Portal, and F. Mollot, *Physica B* **184**, 246 (1993).
- <sup>21</sup>G. S. Vieira, J. M. Villas-Bôas, P. S. S. Guimarães, Nelson Stuard, J. Kono, S. J. Allen, K. L. Campman, and A. C. Gossard, *Phys. Rev. B* **70**, 035316 (2004).
- <sup>22</sup>G. S. Vieira, S. J. Allen, P. S. S. Guimarães, K. L. Campman, and A. C. Gossard, *Phys. Rev. B* **58**, 7136 (1998).
- <sup>23</sup>L. A. Cury, A. Celeste, and J. C. Portal, *Phys. Rev. B* **38**, 13482 (1988).